A Comparison of Two Sonic Anemometers and Fast-Response Thermometers

JOHN E. GAYNOR

NOAA/Wave Propagation Laboratory, Boulder, Colorado

CHRISTOPHER A. BILTOFT

U.S. Army Dugway Proving Ground, Dugway, Utah

10 February 1988 and 25 June 1988

ABSTRACT

In an experiment conducted at the Boulder Atmospheric Observatory (BAO), comparisons were made between two types of sonic anemometer and thermometer systems. One sonic anemometer was a single-axis system manufactured by Campbell Scientific, Inc., (SCI) and the other the type routinely used on the BAO tower. It is similar to the sensors manufactured by Applied Technologies, Inc., and AIR Inc. Two identical Campbell Scientific systems were mounted on each side of the BAO system and comparisons made over a range of atmospheric surface layer conditions. The means and standard deviations of the vertical wind component and temperature, along with the temperature flux from each system, showed good agreement. Important differences in temperature fluctuation data due to the thermocouple filtering are noted. The effect of these differences on the measured heat fluxes and temperature variances is significant and discussed in some detail. It appears that the response of the CSI thermal mass to solar radiation was the major reason for the discrepancies.

1. Introduction

The increasing use of sonic anemometers for fast-response wind sensing in the atmospheric surface and boundary layers is due in large measure to their increased availability, recognized reliability, and decreasing cost. Also, it is becoming clear that mechanical wind sensors, like propellers and bivanes, do not provide adequate frequency response in the surface layer for measurements of the variance of the vertical velocity, σ_w^2. Propeller anemometers measure only 30% to 60% of σ_w^2, depending on stability, and bivanes can sometimes overestimate σ_w^2 by a considerable amount (Finkelstein et al. 1986). Except for a WMO Report (1980) and Finkelstein et al. (1986), essentially no side-by-side comparisons of various sonic anemometers have been reported in the literature. Ours is the first to be performed with the relatively inexpensive and simple device manufactured by Campbell Scientific, Inc. (CSI). We conducted an experiment at the Boulder Atmospheric Observatory (BAO) comparing two CSI single-axis sonic anemometers with one of the sonic anemometers routinely used at the BAO. We discuss statistical comparisons of σ_w^2 and spectral analysis of w to explain similarities and differences in the results. Both systems include a fast-response temperature probe mounted near the vertical path for computing the vertical flux of temperature. Comparisons of temperature variance, σ_T^2, and temperature flux, $\overline{w'T'}$, comparisons are also presented.

2. Instrumentation and experimental setup

The instrumentation and experimental setup have been discussed in a preliminary report by Biltoft and Gaynor (1987). Therefore, only a brief outline is presented here. The BAO instrumentation has been discussed in some detail by Kaimal and Gaynor (1983).

The BAO three-axis sonic anemometer is similar in design to a commercial anemometer manufactured by Applied Technologies, Inc. Each sonic axis contains transmitter/receiver transducer pairs which pulse synchronously 200 times per second. Twenty transit time differences between transducer pairs on each axis are averaged to provide ten samples per second. One of the axes is oriented vertically to measure the vertical wind, w. The other two are horizontal and at 90° with respect to one another.

The Campbell Scientific CA27T units are single-axis analog sonic anemometers. They were oriented vertically and thus sense only the vertical wind component. The acoustic path length is 0.1 m; single transducers at each end are multiplexed to receive alternately and transmit sound pulses. The unit contains a phase lock loop (PLL) circuit to measure the wind speed parallel to the path (Larsen et al. 1979). Because the zero offset in the vertical wind is temperature dependent, these units do not normally provide an absolute measure of w. Each transducer transmits 78 times per second. The

Corresponding author address: Dr. John E. Gaynor, NOAA, Mail Code R/E/WP7, 325 Broadway, Boulder, CO 80303.

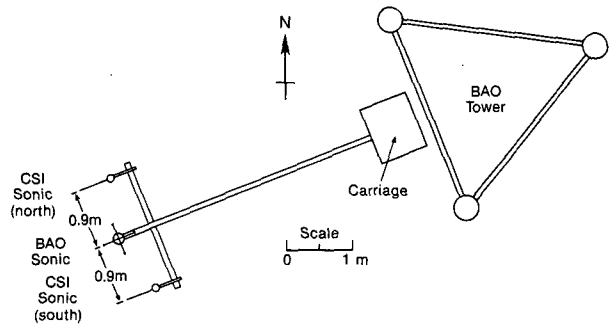

FIG. 1. Configuration of the carriage mount of the Campbell north and south sonics and the BAO sonic on the BAO tower. The view is from above.

analog output is sampled by the BAO data acquisition system at ten samples per second. Unlike the output of the BAO sonics, the output of the CSI sonic is not averaged prior to sampling. Campbell and Unsworth (1979) have presented details of an earlier version of this instrument.

The fast-response temperature sensor mounted near the vertical path of the BAO sonic is an AIR, Inc., Model DTIA platinum wire resistance thermometer. The sensor contains a 12 μm platinum wire with 150 ohm nominal resistance and with a half-power response at approximately 20 Hz, about twice the sampling rate (Kaimal and Gaynor 1983). The CSI sonic contains a 13-μm chromel-constantan thermocouple probe mounted near the sonic path, with a frequency response near 30 Hz, referenced to the thermal mass temperature of the mounting base pivot arm. The thermocouple probe measures the difference between the air temperature and the slowly varying thermal mass temperature of the pivot arm. The measured temperature fluctuations are therefore deviations from a fluctuating reference. Tanner et al. (1985) reported a time constant of 20 min for the reference junction. The BAO fast-response platinum temperature sensor, on the other hand, measures deviations from a fixed mean and therefore provides fluctuations with a high degree of relative accuracy.

Figure 1 shows the relative locations of the sensors on a platform at the end of a boom. The two CSI sonics were mounted 0.9 m north and 0.9 m south of the BAO sonic. (They are hereafter referred to as CSI-north and CSI-south, respectively.) The boom was attached to a movable instrument carriage on the southwest face of the BAO tower. This carriage was moved to 50 m above the ground in all but the last data run, during which it was operated 10 m above the ground. The individual data runs were chosen for steady wind directions that ensured proper exposure to the wind with no shadowing of one sensor by another. Periods were also chosen to reflect varying atmospheric conditions and stabilities. The thermocouple and the platinum wire probes were mounted near the vertical paths of the sonic anemometers.

3. Analysis of the results

Several data runs were made representing surface layer stabilities ranging from slightly stable to moderately unstable conditions. The data runs totaled 8 hours; they were divided into 20-min averaging periods for analysis and statistical comparison.

Although the CSI sonics do not claim a capability for absolute measurement of w, Fig. 2 shows that the two units compared well with the BAO sonic. Scatter plots of 10-s averaged w for a data run under unstable conditions show an approximate -0.2 m s^{-1} bias in CSI-north and CSI-south with respect to the BAO sonics. Table 1 presents the biases for the selected data runs, each about 40 min in length, considered in later analyses. The biases range between approximately -0.1 m s^{-1} and -0.4 m s^{-1}; the Campbell units consistently measure a lower mean than the BAO unit. Some of

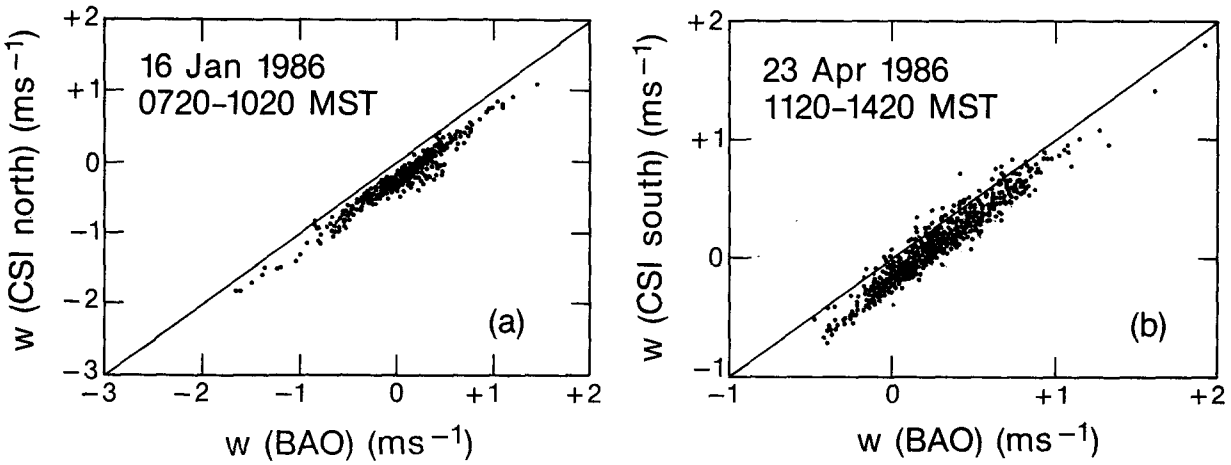

FIG. 2. Scatter plots of the CSI-north sonic 10 s average w vs the BAO sonic for (a) a near-neutral case and (b) an unstable case.

TABLE 1. Biases of the mean vertical velocities between the Campbell sonics and the BAO sonic separated by the individual runs considered.

	(CSI-North) − BAO (m s^{-1})	(CSI-South) − BAO (m s^{-1})
17 Dec.	−0.390	−0.330
	−0.110	−0.060
19 Dec.	−0.275	−0.435
16 Jan.	−0.307	−0.433
	−0.266	−0.412
23 Apr.	−0.209	−0.186
	−0.210	−0.195

the magnitudes of the biases are larger than the 0.2 m s^{-1} maximum offset expected in the BAO sonic w (Skibin et al. 1985). Scatter plots of temperature (not shown) indicate a much larger scatter as well as bias, because the CSI sensor measures temperatures referenced to the slowly varying thermal mass temperature of the mounting base.

Figure 3a presents a scatter plot of σ_w^2. The variances were calculated over 20 min time blocks from data sampled at 10 Hz. The scatter is reasonably small, and the overall agreement quite good. However, the σ_T^2 values calculated over the same 20 min time block (Fig. 3b) show poor agreement.

One would expect the time constant on the CSI thermocouple reference junction to act as a high-pass filter on the data, yielding a lower σ_T^2 than that obtained from the BAO platinum wire. However, in many cases the apparent thermal lag and phase shifts of the CSI reference caused the estimates to be higher.

The plot of the temperature flux, $\overline{w'T'}$, in Fig. 3c shows fairly large scatter but not as large as that for σ_T^2 (Fig. 3b).

The points calculated from a case run on 16 January are shaded in Figs. 3b and 3c. Although not all the points for this day are unusual outliers, it is shown here that this case illustrates the large thermal response of both CSI sensors' thermal masses to external changes in the solar radiation.

To quantify the comparisons, we use the following simple statistics:

$$\text{BIAS} = (\overline{C - B}) \tag{1}$$

and

$$\text{rms} = \{\overline{[(C - \bar{C}) - (B - \bar{B})]^2}\}^{1/2}, \tag{2}$$

where C and B represent the individual 20 min averages of quantities derived from the CSI units and the BAO unit, respectively. Table 2 presents the statistical summary of the comparisons of σ_w^2, σ_T^2, and $\overline{w'T'}$ for all cases. Not surprisingly, the agreement for σ_w^2 is quite good, but agreement for $\overline{w'T'}$ and σ_T^2 is poor. The rms differences in σ_w^2 are about 10% of the means with essentially no bias. For σ_T^2 and $\overline{w'T'}$, the rms differences are the same magnitude as the means, and the biases are significant.

Figure 4 presents frequency spectra and cospectra of w and T for a case on 1220–1340 MST 23 April 1986. Each spectrum was calculated from a time series 80 min long. This case represents a moderately unstable period. The w spectrum (Fig. 4a) shows good agreement with a stronger tendency in the CSI w spectra to turn up at the high end. This feature occurs to varying degrees in all the cases we inspected and appears to be the effect of aliasing (Kaimal et al. 1968). Recall that the CSI sonic measurements are not subjected to prior averaging, whereas the BAO sonic measurements are each averages of 20 consecutive nonoverlapping points. Aliasing has no significant effect on calculations of the variances and covariances. The good agreement in the spectra in the middle to lower frequencies (Fig. 4a) also occurs in the other cases.

The T spectra in Fig. 4b shows somewhat poorer agreement than those for w. There is some disagreement in the lower frequency portion of the T spectra. This disagreement occurs in varying degrees in the spectra for the other cases also. The differences between

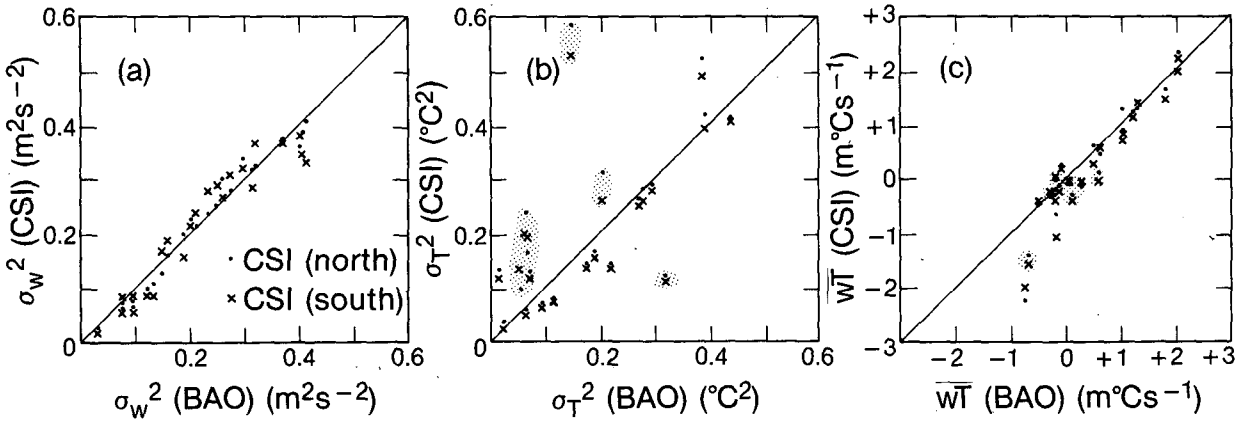

FIG. 3. Scatter plots for all cases of (a) σ_w^2, (b) σ_T^2, and (c) $\overline{w'T'}$. The shaded areas in (b) and (c) represent the 16 January case.

TABLE 2. Statistical comparisons of Campbell and BAO sensors compiled from 24 separate 20-min runs (all stabilities).

Parameter	Mean			Bias		Rms	
	CSI-North	CSI-South	BAO	(CSI-North − BAO)	(CSI-South − BAO)	(CSI-North − BAO)	(CSI-South − BAO)
σ_w^2 ($m^2 s^{-2}$)	0.215	0.218	0.215	0.0	0.002	0.022	0.032
σ_T^2 ($°C^2$)	0.496	0.476	0.573	−0.077	−0.097	0.326	0.337
$\overline{w'T'}$ (°C m s^{-1})	0.023	0.017	0.035	−0.012	−0.018	0.039	0.028

the BAO and CSI T spectra are consistent with the scatter of the temperature variance in Fig. 3b. They are also consistent with our earlier hypothesis that thermal lag in the CSI reference can artificially increase or decrease the measured σ_T^2. Whether the combined high-pass filtering and thermal lag effects at the CSI T reference junction increase or decrease the lower frequency contribution to the total variance of T depends on the ambient temperature signal and on the solar radiation incident on the CSI thermal mass. The drop in the energy in the low-frequency portion of the Campbell T spectrum in Fig. 4b is typical of most runs and consistent with the 20 min high-pass filtering claimed by the manufacturer.

At the high-frequency end, Fig. 4b shows some aliasing in the T spectra for the CSI and BAO sensors. This occurred in varying degrees in all the cases inspected. Recall that the response frequency of the CSI thermocouple is about 30 Hz, slightly faster than that of the BAO platinum resistance thermometer. Neither the CSI nor the BAO temperature readings were averaged prior to sampling. It is reassuring to note that neither the conductivity nor thermal boundary layer effects discussed by Lecordier et al. (1981) are evident in the BAO and CSI T spectra at frequencies up to 5 Hz.

The cospectra of w and T are shown in Fig. 4c for the same cases as in Figs. 4a and 4b. The area under the curves in Fig. 4c equals the temperature flux in the frequency band. Where the departure in the low-frequency energy was the largest in the T spectrum (Fig. 4b), the differences in the cospectra in Fig. 4c are also larger. However, the general agreement is better than in Fig. 4b and this is consistent with the scatter in Fig. 3b, c.

The coherence and phase between the CSI and BAO temperatures for the two cases are presented in Fig. 5a, b, respectively. (The 16 January case has not been included in this figure because of its unusual characteristics.) On each graph, the abscissa is plotted in terms of a horizontal wave number (inverse wavelength), f/U, where U represents the mean horizontal wind component. Figure 5 presents two runs that were long enough in time for spectra to be calculated on two separate days, representing a stable surface layer (17 December) and a convective surface layer (23 April). The coherence curves in Fig. 5a collapse very well for the two runs. Both cases show the coherence dropping to zero at a scale around 5 m and smaller. This drop, attributed to sensor separation, was anticipated. However, the coherence drop at the larger scales (smaller wave numbers) is unusual. There would be no drop if all three instruments were responding identically to the low-frequency variations in temperature. The coherence between them should be unity at large scales. The fact that the coherence becomes small in this region seems clearly a consequence of degraded response due to the thermal lag in the CSI reference junction. The phase plot in Fig. 5b shows a shift away from 0°/360° in both directions at the low wave numbers. The phase

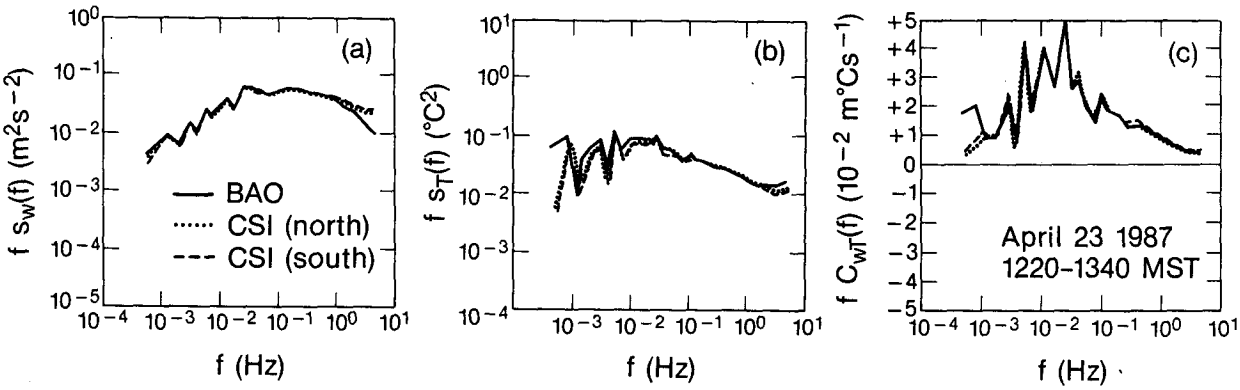

FIG. 4. (a) Spectra of vertical velocity (w), (b) temperature (T), and (c) cospectra of w and T for the case of 23 April 1986, 1220–1340 MST.

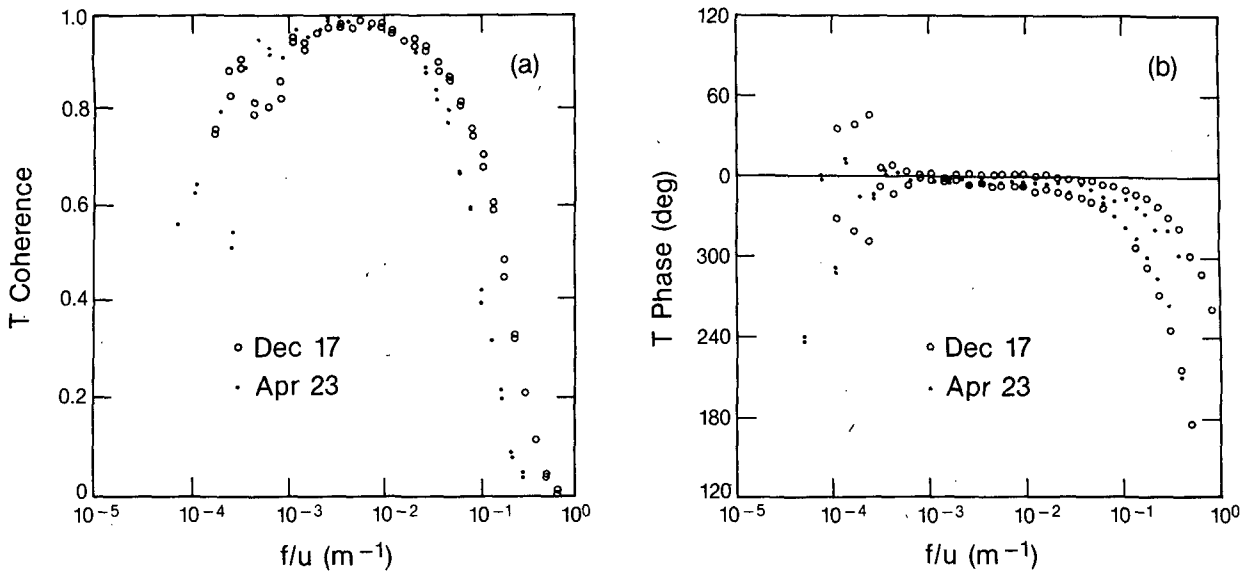

FIG. 5. (a) Coherence and (b) phase angle between the Campbell and BAO temperatures.

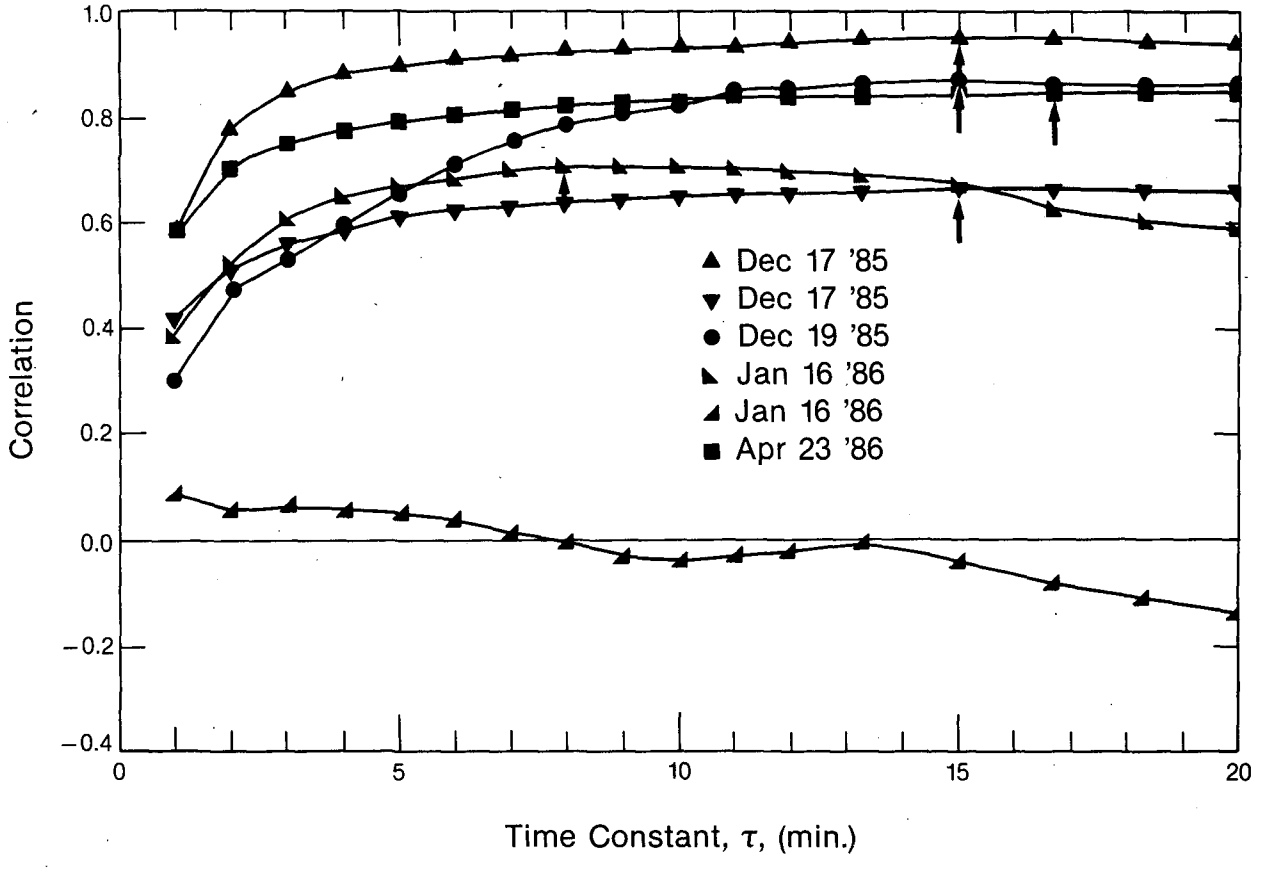

FIG. 6. Correlation between the Campbell and BAO temperature sensors vs the filter lag window applied to the BAO temperature time series.

shift at higher wave number end is consistent with the coherence drop at that end.

It appears, therefore, that the CSI thermocouple reference junction cannot be treated as a simple high-pass filter. If it were such a filter, the T spectra and the phase shifts would behave more predictably at the low-frequency end. External factors such as changes in wind speed and solar radiation must influence the reference junction temperature and these cannot, in general, be represented by a simple function. Biltoft and Gaynor (1987) high-pass filtered both the CSI and BAO temperatures with a 60 s time constant and found substantial improvement in the comparisons of σ_T^2 and $\overline{w'T'}$. Although this filter successfully eliminated phase shifts and low frequency drifts in the CSI temperatures, it also eliminated some of the natural temperature fluctuations contributing to these quantities.

However, it is useful to subject the BAO sonic data

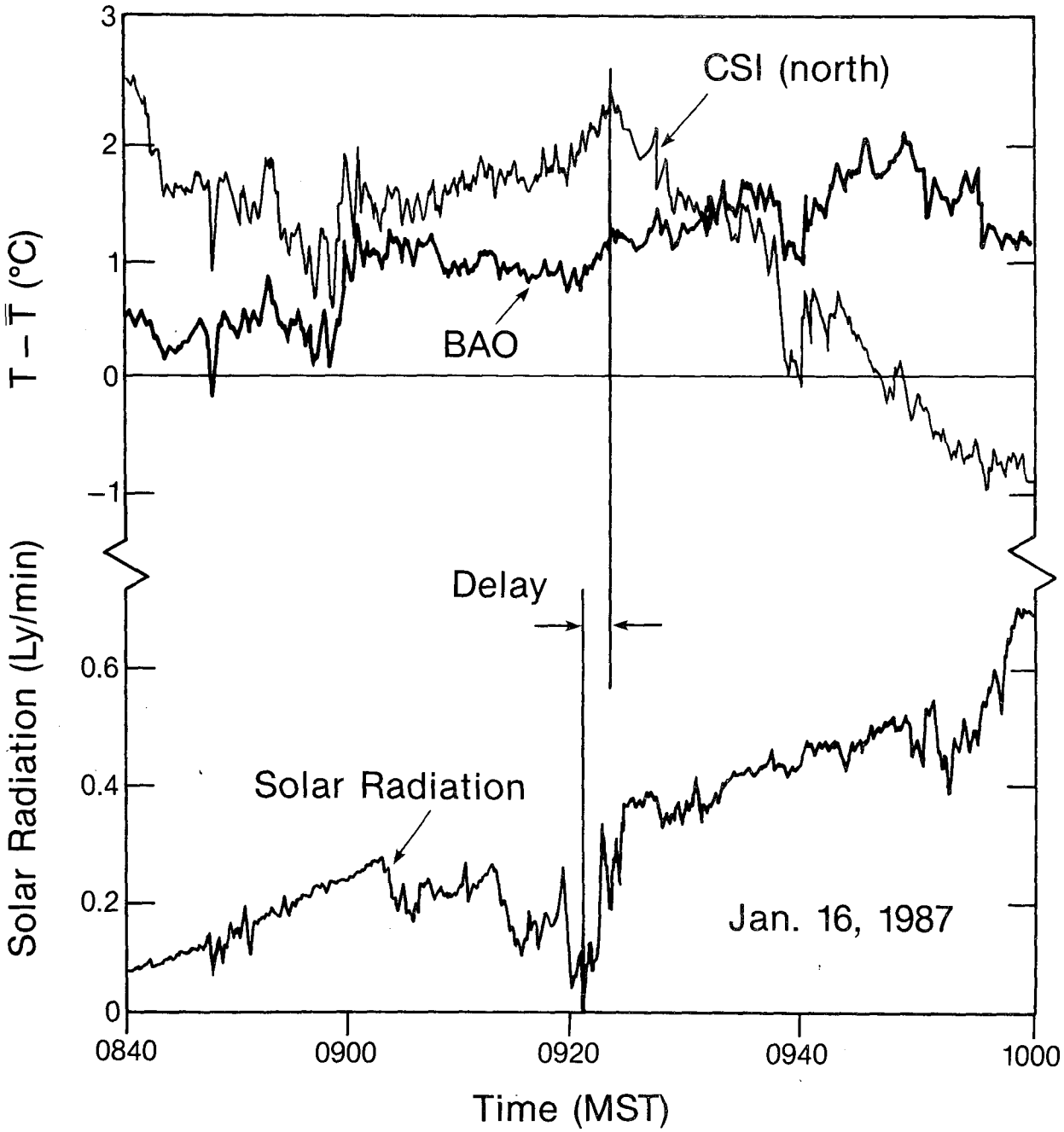

FIG. 7. Time series of the CSI-north and BAO temperature sensors, with means removed, and the incoming shortwave solar radiation for the 16 January case.

to filters with varying time constants and simulate the effect of the CSI thermal mass on the measured time series. Cross-correlating the two should provide us an estimate of the thermal lag in the CSI reference junction.

For this test, a simple exponential moving filter was differenced from the original BAO time series. The high-pass filtering can be represented by

$$(x)_{\text{filtered}} = x - \left(\sum_{i=1}^{n} x_{n+1-i} e^{-i\Delta t/\tau} \Big/ \sum_{i=1}^{n} e^{-i\Delta t/\tau}\right), \quad (3)$$

where $\Delta t = 10$ s and τ, the filter time constant ($1/e$ point) was varied from 0.5 min to 20 min. These high-pass filtered time series, with varying τ, were then correlated with the corresponding CSI temperature series. The results are presented in Fig. 6. Each curve represents the average of north and south CSI sensors since the two were practically the same. The τ for which the correlation is a maximum should correspond to the thermocouple lag. The peaks in the correlation are very broad and somewhat difficult to locate in Fig. 6. The arrows indicate approximate locations of the peaks. The peaks appear to cluster around $\tau \approx 15$ min, except in the 16 January case. The broad peaks and varying maximum correlations in each case indicate that this simple filter does not simulate very well all the ambient effects on the thermal mass.

The 16 January time series, particularly the latter half of the period, stands out as an extreme example. The correlation hovers around zero. In the scatter diagrams of Fig. 3b, c, this case shows the worst agreement (note the shaded areas). Figure 7 helps explain the probable reason for the disagreement between the filtered BAO data and the CSI data. Here, original unfiltered time series from the BAO sensor and CSI-north are plotted (with their means removed) for the entire period analyzed on that day. (The trace from CSI-south was identical to that from CSI-north.) We see a large trend in the CSI-north temperature trace not apparent in the BAO trace. The onset of this large trend lags, by about 2 min, a sudden increase in the incoming shortwave solar radiation measured by an Epply pyranometer at the BAO site. Because the CSI temperatures are differences from the thermal mass temperature, it appears that the reference temperature rose in response to the sudden increase in the solar radiation, causing the output temperature to drift in the negative direction. Clearly, no simple filter can anticipate this drift.

4. Summary and conclusions

Comparisons of the CSI sonics with the BAO sonic showed excellent agreement for the fluctuating vertical wind component. The agreement of averaged w was also reasonably good. This was surprising since CSI does not make claims for accuracy in the mean w for run lengths over runs longer than 10 min.

The comparison deserving most attention is that of the temperature sensors. As with the resistance temperature sensor on the BAO unit, this fast-response sensor is designed for use in conjunction with w for computing σ_w^2 and $\overline{w'T'}$. The differences between these quantities derived from the Campbell thermocouples and the BAO platinum resistance unit were significant. The cause of these large differences was the combined effects of the high-pass filtering provided by the thermal mass reference in the presence of shifts in the incoming solar radiation.

A simple exponential high-pass filter was applied to the BAO temperature time series in an attempt to simulate the response at the CSI reference junction. The results confirmed that the response is not a simple function. These results point to the necessity of either using a much larger thermal mass, or carefully insulating the thermal mass to increase its time constant. Preliminary tests indicate that increasing the time constant of the mass by as long as 1 hour improved the temperature signal. Further tests are needed to establish how well the statistics compare with a standard temperature fluctuation sensor.

REFERENCES

Biltoft, C. A., and J. E. Gaynor, 1987: Comparison of two types of sonic anemometers and fast response thermometers. Preprints, *Sixth Symp. on Meteorol. Observation and Instrumentation,* January 12–16, New Orleans, Louisiana, Amer. Meteorol. Soc., 173–176.

Campbell, G. S., and M. H. Unsworth, 1979: An inexpensive sonic anemometer for eddy correlation. *J. Appl. Meteor.*, **18,** 1072–1077.

Finklestein, P. L., J. C. Kaimal, J. E. Gaynor, M. E. Graves and T. J. Lockhart, 1986: Comparison of wind monitoring systems. Part I: In situ sensors. *J. Atmos. Oceanic Technol.*, **4,** 583–593.

Kaimal, J. C., and J. E. Gaynor, 1983: The Boulder Atmospheric Observatory. *J. Appl. Meteor.*, **22,** 863–880.

——, J. C. Wyngaard and D. A. Haugen, 1968: Derived power spectra from a three-component sonic anemometer. *J. Appl. Meteor.*, **7,** 827–837.

Larsen, S. E., F. W. Weller and J. A. Businger, 1979: A phase-locked loop continuous wave sonic anemometer-thermometer. *J. Appl. Meteor.*, **18,** 562–568.

Lecordier, J. C., P. Paranthoen and C. Petit, 1981: The effect of the thermal prong-wire interaction on the response of a cold wire in gaseous flows (air, argon and helium). Preprints, *Seventh Biennial Symp. on Turb.*, Rolla, Missouri, 21–23 September, Amer. Meteor. Soc., Chapter 26.

Skibin, D., J. C. Kaimal and J. E. Gaynor, 1985: Measurement errors in vertical wind velocity at the Boulder Atmospheric Observatory. *J. Atmos. Oceanic Technol.*, **2,** 598–604.

Tanner, B. D., M. L. Tanner, W. A. Dugas, E. C. Campbell and B. L. Bland, 1985: Evaluation of an operational eddy correlation system for evapotranspiration measurements. *Proceedings of the National Conference on Advances in Evapotranspiration,* December 16–17, 1985, Chicago, IL., American Society of Agricultural Engineers Publication 14-85, 16 pp.

World Meteorological Organization, 1980: Instruments and Observing Methods, Report No. 3, Lower Tropospheric Data Compatibility, Low-Level Intercomparison Experiment. Boulder, CO (USA), 20 August–6 September 1979. Secretariat of the World Meteorological Organization, Switzerland, 190 pp.